International Congress on Evolutionary Methods for Design,
Optimization and Control with Applications to Industrial Problems
EUROGEN 2003
G. Bugeda, J.A.- Désidéri, J. Periaux, M. Schoenauer and G. Winter (Eds)

MULTI–OBJECTIVE DESIGN OF OPTIMAL COMBINED CYCLE POWER PLANTS WITH SUPPLEMENTARY FIRING

Eleni T. Bonataki[⋆], Alexis P. Giotis[†], and Kyriakos C. Giannakoglou[†]

[⋆] (1) Public Power Corporation,
Thermal Projects Engineering & Construction Department,
30-32 Aristotelous Str., Athens 104 33, GREECE,
Tel: (30)-210.823.15.99, Fax: (30)-210.823.01.25,
e-mail: ebonataki@dmkt.dei.gr

[†]National Technical University of Athens,
Lab. of Thermal Turbomachines,
P.O. Box 64069, Athens 157 10, GREECE,
Tel: (30)-210.772.16.36, Fax: (30)-210.772.37.89,
e-mail: [agiotis , kgianna]@central.ntua.gr ,
http://velos0.ltt.mech.ntua.gr/EASY

Key words: Evolutionary Algorithms, Multi–objective Optimization, Constraints, Energy, Combined Cycle Gas Turbine Power Plants, Supplementary Firing.

Abstract. *This paper is dealing with the design of an optimal combined cycle power plant with supplementary firing. For this purpose, an Evolutionary Algorithm based optimization tool, namely code* EASY 1.3 *developed by the National Technical University of Athens, will be used to carry out a number of different optimizations. The main target is to get configurations with maximum efficiency and power output at minimum cost. Such a three-objective optimization yields a* 3*D Pareto surface; this has been analyzed in detail by running additional two–objective cases and scrutinizing their results. The analysis of the obtained results offers a complete understanding of the role of various design parameters, including supplementary firing.*

1 INTRODUCTION

Electric power generation using both gas and steam turbines, operating in combined cycle, is nowadays in widespread use. It is well known that Combined Cycle Gas Turbine ($CCGT$) power have short erection time, low investment cost and particularly higher efficiency compared to that of conventional steam power plants. Building optimal $CCGT$ power plants requires first to define the design parameters and then to employ an optimization method with one or more objectives. Maximizing power output as well as efficiency while minimizing the capital cost are three typical targets.

This paper is dealing with the design of an optimal $CCGT$ plant with supplementary firing, shown in fig. 1. Supplementary firing (sf) is used at the gas turbine exit (position 0) in order to increase the temperature of exhaust gases entering the Heat Recovery Steam Generator ($HRSG$), in the expense of additional fuel consumption.

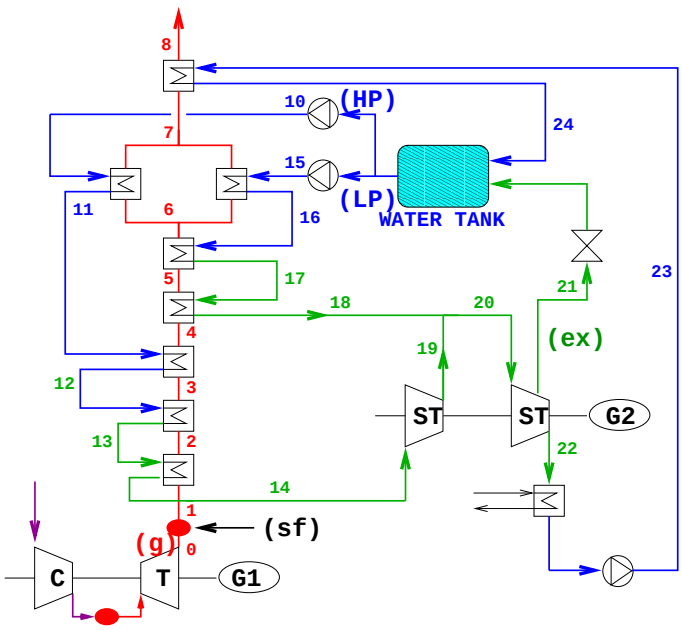

Figure 1: Combined Cycle Gas Turbine Power Plant with Supplementary Firing.

The design of an optimal power plant calls for multi-criteria optimization tools and Evolutionary Algorithms (EA) is an evident choice. In this paper, the use of the optimization software *EASY 1.3* (*Evolutionary Algorithm SYstem*, developed by the Lab. of Thermal Turbomachines of the National Technical University of Athens) for a realistic design will be demonstrated. *EASY 1.3* is capable of handling both single– and multi–objective, constrained or unconstrained optimization problems and may also reduce the number of required evaluations through the use of surrogate models, such as artificial neural networks. Most of the theoretical aspects and the capabilities of *EASY 1.3* are

analyzed in [1] and [2].

2 THE COMBINED CYCLE GAS TURBINE POWER PLANT

The *CCGT* power plant that will be optimized is shown in fig. 1. During the design process some of the operating parameters are considered to take on fixed (user–defined) values. The fixed parameters are:

- the gas turbine operating data, namely the power output (70 MW), efficiency (40%), exhaust gas mass flow rate (265 kg/s) and temperature (440^oC),
- efficiencies (isentropic 90% for the *HP* and 87% for the *LP*, mechanical $\eta_{mech} = 90\%$ and electrical η_{el}=100%) related to the steam turbine (*ST*) and its generator (*G2*),
- the extraction pressure (2.5 bar, marked by *ex* in fig. 1) from the *LP* steam turbine and
- the condenser vacuum (45 $mbar$, position 22), which is chosen for minimal waste heat in the condenser.

The design variables, i.e. the parameters controlled by the optimization tool are listed below. The lower and upper bounds $[Lower, Upper]$ for the most important among them are also given. Some of the unknown temperatures are indirectly defined as differences from other temperatures computed during the power plant analysis.

- the *HP* steam pressure $[20, 100\ bar]$,
- the *LP* steam pressure $[2, 15\ bar]$,
- the superheated steam temperature at the exit of the *HP* branch of the *HRSG* (position 14), defined as the difference from the exhaust gas temperature after the supplementary firing,
- the feedwater temperature at the inlet (position 12) to the *HP* evaporator,
- the feedwater temperature at the exit (position 11) from the first *HP* economizer,
- the feedwater temperature at the inlet (position 16) to the *LP* evaporator,
- the superheated *LP* steam temperature (position 18),
- the total pressure of steam driven to the water tank $[1.1, 2.0\ bar]$,
- the percentage r of the flue gases mass flowrate that passes through the *LP* economizer $[10\%, 45\%]$,

- the flue gases temperature at the condensate preheater inlet (position 7),
- the *HRSG* exhaust (position 8) gas temperature $[103, 110^oC]$ and
- the supplementary fuel mass flowrate $\dot{m}_{sf}$, expressed as the percentage of O_2, contained in the flue gases at position 0 and used for the supplementary firing, $[0\%, 100\%]$

According to the *EA* terminology, the thermal analysis of a *CCGT* power plant requires the so–called evaluation tool. This is based on a system of mass and heat balance equations, governing the various plant components. These equations are summarized below. H and h will denote flue gases and water/steam enthalpies, respectively; LHV_{fuel} is the lower heating value of the fuel (natural gas):

(a) Heat balance occurring in the *HRSG* heat exchangers (below, this is written only for the heat exchangers located between positions 6 and 7):

$$\begin{aligned} r(\dot{m}_g + \dot{m}_{sf})(H_6 - H_7) &= \dot{m}_{LP}(h_{16} - h_{15}) \\ (1-r)(\dot{m}_g + \dot{m}_{sf})(H_6 - H_7) &= \dot{m}_{HP}(h_{11} - h_{10}) \end{aligned}$$

(b) Heat balance occurring in the condensate preheater:

$$(\dot{m}_g + \dot{m}_{sf})(H_7 - H_8) = (\dot{m}_{HP} + \dot{m}_{LP} - \dot{m}_{ex})(h_{24} - h_{23})$$

(c) Heat balance occurring in the feedwater tank:

$$\dot{m}_{ex}(h_9 - h_{25}) = (\dot{m}_{HP} + \dot{m}_{LP} - \dot{m}_{ex})(h_{24} - h_9)$$

(d) Work–heat balance occurring in the steam turbine:

$$\begin{aligned} P_{ST} &= (\dot{m}_{HP}(h_{14} - h_{19}) + (\dot{m}_{HP} + \dot{m}_{LP})(h_{20} - h_{21}) \\ &+ (\dot{m}_{HP} + \dot{m}_{LP} - \dot{m}_{ex})(h_{21} - h_{22}))\eta_{el}\eta_{mech} \end{aligned}$$

(e) Heat balance occurring in supplementary firing:

$$(\dot{m}_g + \dot{m}_{sf})H_1 = \dot{m}_g H_0 + \dot{m}_{sf} LHV_{fuel}$$

The thermodynamic properties of flue gases, water and steam are all modelled using polynomial expressions. The flue gases composition after the supplementary firing (position 1) is calculated using combustion equations. The total efficiency of a *CCGT* power plant is given by

$$\eta_{CC} = \frac{P_{GT} + P_{ST}}{\dot{m}_{fuel} LHV_{fuel}}$$

where P_{GT} and P_{ST} is the electrical power produced at the gas and steam turbines respectively and $\dot{m}_{fuel}$ is the total fuel mass flowrate.

The capital cost of the *CCGT* plant is calculated by summing up the cost of its main components, viz. the gas turbine, the *HRSG* system and the steam turbine as well as the cost of the additional electromechanical equipment and civil works which are necessary in order to complete the plant (expressed as a fixed percentage of the main equipment cost). The cost of gas and steam turbines depends upon the power of each one of them. In order to compute the cost of the *HRSG* system, the total area of the heat exchangers of the *HRSG* is required.

Finally, for the *HRSG* of this power plant, twelve inequality constraints should be fulfilled in order to ensure feasible heat exchanger design. Additionally, the inlet temperature to the steam turbine (position 14) should not exceed 565^oC. All these inequality constraints are taken into account by penalizing the cost value of all the objectives. Practically, for any inequality constraint of the form $T_a \geq T_b$, if $\Delta T = T_a - T_b < 0$, the penalty factor $p_i = e^{\Delta T / T_b}$ is computed. The total penalty factor p_{tot} is the product of all p_i's and the penalized cost value is the $y_k = y_k / p_{tot}$.

Having defined objectives and constraints, we seek to optimize the relevant Rankine cycle and the heat-temperature ($Q - T$) diagram for the *HRSG*. In the $Q - T$ diagrams that will be shown in the Results section for a number of optimal configurations, flue gases and (counter–flowing) water or steam temperatures will be plotted and the constraints will be interpreted graphically.

3 EVOLUTIONARY ALGORITHMS

One of the fundamental application of Evolutionary Algorithms (*EA*) is as optimization tool. *EA* process populations of candidate solutions rather than single individuals. A selection process and a probabilistic random variation are the main features of any *EA*. Implicit to the selection process is one or more objective functions, used to determine the cost or merit of each population member with respect to an equal number of targets. The most frequently used variants of *EA*, i.e. Genetic Algorithms (*GA*) and Evolution Strategies (*ES*) are described in many standard textbooks, [3], [4], [5].

The *EASY 1.3* optimization software constitutes a generalization of *GA* and *ES* with several add–on features and, for this reason, it will be referred to as an Evolutionary Algorithm.

Before describing the K–objective *EA* built in *EASY 1.3*, a couple of notations should be introduced. The decision vector will be denoted by $\overrightarrow{x}^{(i)}$ and its components by $x_m^{(i)}$, $m = 1, M$. The corresponding objective vector is $\overrightarrow{y}^{(i)}$, with components $y_k^{(i)}$, $k =$

$1, K$. The objective functions represent the mapping $\Re^M \rightarrow \Re^K$. In minimization problems, the decision vector $\overrightarrow{x}^{(p)}$ dominates $\overrightarrow{x}^{(q)}$ ($\overrightarrow{x}^{(p)} < \overrightarrow{x}^{(q)}$) if and only if $\forall\ k \in [1, K]$: $y_k^{(p)} \leq y_k^{(q)}$ and $\exists\ k \in [1, K] : y_k^{(p)} < y_k^{(q)}$.

Using a notation which is common in *ES*, [5], we will denote any *EA* that will be used in this paper by (μ, κ, λ); this symbol denotes the evolution from the parent population of μ individuals to the offspring population of λ individuals, while allowing maximal life span of individuals equal to κ generations. Also, if g stands for the generation counter, then $S^{g,\mu}$ and $S^{g,\lambda}$ will denote the set of parents and offspring in the g-th generation. From the algorithmic point of view, the aim of an *EA* to compute the Pareto front of optimal solutions in $\Re^K$ is equivalent to the use of the archival front $S^{g,a}$. Upon convergence, $S^{g,a}$ contains the set of nondominated solutions to the K-objective problem. From a more general point of view, the role of $S^{g,a}$ is to preserve elitism during the evolution. It is for this reason that, in *EASY 1.3* an archival front $S^{g,a}$, with more than one solutions, is also maintained in single–objective problems. The maximum size α of $S^{g,a}$ is a user–defined parameter.

4 THE MULTI–OBJECTIVE EVOLUTIONARY ALGORITHM

The major steps of the multi–objective *EA* are given below:

Step 1: The λ individuals $\overrightarrow{x}^{(i)} \in S^{g,\lambda}$, either created during the previous generation or selected at random (at the first generation), undergo evaluations; so, values are given to the objective vectors

$$\overrightarrow{y}^{(i)} = F\left(\overrightarrow{x}^{(i)}\right) \quad ; \quad \overrightarrow{x}^{(i)} \in S^{g,\lambda} \tag{1}$$

Step 2: The nondominated individuals belonging to $S^{g,\lambda} \cup S^{g,\alpha}$ are identified. These form the provisional Pareto front $S^{g+1,\alpha*}$. It is the first action taken in order to preserve elitism in the population. If $S^{g+1,\alpha*}$ is overcrowded (with respect to the aforementioned α value), a thinning process will be employed in Step 4. The role of thinning will be to reduce the size of $S^{g+1,\alpha*}$ and create $S^{g+1,\alpha}$ with better point distribution.

Step 3: Using the values of $\overrightarrow{y}^{(i)}$, $i \in S^{g,\mu} \cup S^{g,\lambda} \cup S^{g+1,\alpha*}$, a unique cost value $\phi^{(i)}$ per individual is computed. Of course, in maximization problems, $\phi^{(i)}$ will be referred to as fitness value. Through the cost (or fitness) assignment, standard single–objective evolution operators can be used. There is a large literature on the subject of cost (or fitness) assignment ([6], [7], [8], [9], [10], [11], to mention only some of the most notable works). They are all based on domination criteria and the concept of the Pareto front; most of these methods also locate and penalize clustered solutions, in order to promote diversity. Among the many algorithmic variants offered to the users of *EASY 1.3*, the two most inportant are listed below. Note that, with

respect to the standard forms of these algorithms (see the works cited below) certain modifications were necessary for adapting them to the (μ, κ, λ) scheme.

- *Front ranking based methods*: The $S^{g,\mu} \cup S^{g,\lambda} \cup S^{g+1,\alpha*}$ members are ranked in fronts using a repetitive procedure. Note that the first front (front 0) of the absolutely nondominated solutions is already known ($S^{g+1,\alpha*}$). The members of front 0 are initially given the same lowest ϕ value. Then, in order to promote diversity, these values are penalized using sharing functions according to the niching concept. Distances can be measured either in the decision variables' or the objectives' space. The cost assignment algorithm ensures that the ϕ value of any individual of the j-th front is greater than the highest ϕ value of the $(j-1)$-th front. This method is conceptually similar to the one proposed in [6], with the previously discussed modifications.
- *Strength based methods*: This variant is based on the algorithms introduced in [10], [11]. All the $S^{g+1,\alpha*}$ members are first assigned a cost value equal to the number of the $S^{g,\mu} \cup S^{g,\lambda}$ individuals they dominate, divided by $\mu+\lambda+1$. Then, the ϕ value of each of the $S^{g,\mu} \cup S^{g,\lambda}$ members is set equal to 1 plus the sum of strengths of the $S^{g+1,\alpha*}$ individuals which dominate it. Other algorithmic variants are also possible. For instance, likely [11], strengths can be computed for all the $S^{g,\mu} \cup S^{g,\lambda} \cup S^{g+1,\alpha*}$ members; then, the ϕ value for each one of them is the sum of strengths it dominates. The final ϕ value is the sum of the previously computed value plus a contribution proportional to the local density of individuals. This is calculated from the distance of this individual from its k-th closer neighbour, measured in the objectives' space.

Step 4: The archival front $S^{g+1,\alpha}$ of the current generation is formed. If the size of $S^{g+1,\alpha*}$ is less than the user–defined parameter α, the nondominated solutions of $S^{g+1,\alpha*}$ are merely copied to $S^{g+1,\alpha}$; in contrast to some other methods (such as $SPEA2$, [11]), $S^{g+1,\alpha}$ consists only of nondominated individuals, so its size might be less than α. On the other hand, if $S^{g+1,\alpha*}$ contains more than α members, an iterative thinning process, that eliminates one of its members at a time, is employed. In each iteration, the individual to be eliminated is selected between the two members of $S^{g+1,\alpha*}$ with minimum distance in the objective space, the criterion being the second smaller distance from its neighbours. This algorithm (described also in [11]) is simple and fast as long as a reasonably low value of α is utilized. An important feature of this algorithm is that it maintains the Pareto front extent, i.e. it does not eliminate the individuals lying along the edges of the archival front.

Step 5: Aiming at preserving elitist solutions in the active population sets (second application of elitism), a small fraction of the topmost solutions of $S^{g+1,\alpha}$ are copied directly to $S^{g,\lambda}$, by replacing an equal number of the worse individuals in this set. $S^{g,\lambda}$ is, practically, overwritten.

Step 6: The new $S^{g+1,\mu}$ set of possible parents is created from the $S^{g,\lambda} \cup S^{g,\mu}$ individuals. First, the $S^{g,\mu}$ individuals that have reached the maximum allowed life span are eliminated from $S^{g,\mu}$. Then, the members of $S^{g,\lambda} \cup S^{g,\mu}$ are rank sorted in terms of their ϕ values and the μ top individuals are selected to form the new $S^{g+1,\mu}$ set.

Step 7: The new offspring set $S^{g+1,\lambda}$ is created by appling the parent selection operators to the $S^{g+1,\mu} \cup S^{g+1,\alpha}$ superset. Parent individuals are randomly selected from $S^{g+1,\mu}$ (with probability p_{ps}) or $S^{g+1,\alpha}$ (with probability $1 - p_{ps}$). If $\mu < \lambda$, the aforementioned random selection is adequate. But, whenever $\mu \geq \lambda$, additional selective pressure should be exerted by increasing the possibility of selecting parents with lower cost values; for instance, schemes such as the probabilistic tournament selection scheme are used. The number of candidates participating in the tournament and the probability of selecting the candidate with the smaller cost value are user–defined parameters. This is an important difference compared to *SPEA2*, where parents are selected only from $S^{g+1,\alpha}$. Once two parents have been selected, recombination and mutation operators are applied to create a new offspring to be inserted into $S^{g+1,\lambda}$. *EASY 1.3* allows a variety of multi–parent recombination operators to be used.

Step 8: Set $g := g + 1$ and return to Step 1 until a stopping criterion is met. The usual stopping criterion is the maximum number of evaluations.

One of the possibilities offered by the *EASY 1.3* software is the use of surrogate evaluation models (often referred to as *metamodels* or approximate models), [1] and [2]. *EASY 1.3* implements the so–called *Inexact Pre–Evaluation* phase to reduce the number of evaluations required from the same solution quality. In the present analysis, there was no need to use the metamodel, since the evaluation tool was very fast.

5 RESULTS – DISCUSSION

Extending previous work by the authors, [12], this paper will focus on the design of the *CCGT* power plant with supplementary firing, fig. 1. We recall that the goal is to design power plants with maximum efficiency, maximum power output (at *G2*; the power output at *G1* is determined by the gas turbine characteristics) and minimum investment cost. The design variables, the fixed parameters and involved constraints have been discussed in previous sections.

In fig. 2, the Pareto fronts computed through four optimization runs are shown. This $3D$ plot includes one Pareto front (surface, formed by a cloud of points) from a three–objective optimization and three Pareto fronts ($3D$ curves) resulted from three two–objective optimizations. For the latter, the objectives were (a) *max.efficiency–max.power*, (b) *max.efficiency–min.cost* and (c) *max.power–min.cost*. In each one of them, the third objective was not considered and the corresponding values were post–computed just to facilitate the inclusion of the derived solutions into the $3D$ plot. Of course, all of the

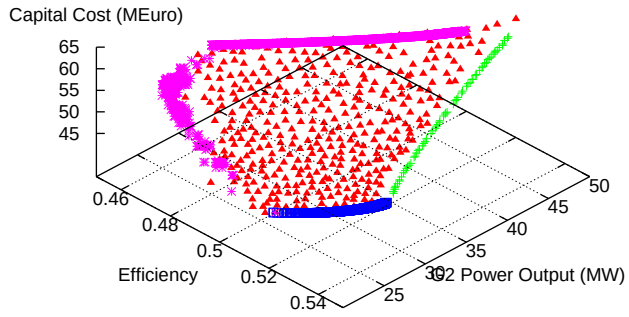

Figure 2: Results form one three-objective and three two–objective optimizations, shown in the $3D$ space of objectives. The three two-objective runs define the bounds of the Pareto surface,i.e. the outcome of the three-objective optimization.

constraints have been taken into account. As expected, the three two–objective fronts constitute the bounds of the Pareto surface. In fig. 2, they correspond to the (a) right, (b) bottom and (c) top-left bounds of the Pareto surface, respectively. Fig. 2 indicates also the lower and upper values of the three objective functions for the optimal solutions. So, efficiency varies between 45% and 55%, power between 19 and 51 MW and cost between 45.5 and 66.5 $MEuro$, approximately.

It is interesting to interpret the type of solutions captured by the two–objective runs. For this reason, fig. 3 shows three $2D$ plots (each one with different axes, i.e. all the possible combinations). The three–objective results are omitted but it is clear that they cover the area between the three two–objective Pareto fronts. The *max.efficiency–max.power* optimization yields (on the corresponding plane) an almost linear front at the highest efficiency levels (between 52% and 55%, respectively). The higher efficiencies correspond to lower power levels (from 50 to 26 MW), respectively. Cost and power remain proportional; we recall that since the cost was not included in the objectives, the demand for maximum power leads to high investment costs (> 55 $MEuro$). The outcome of the *max.efficiency–min.cost* optimization is a front located also in the high efficiency area. Finally, the *max.power–min.cost* design yields a Pareto front which is differently shaped in the three plots. Though on the *power–cost* plane this is a monotone curve, on the other two planes the same efficiency can be achieved with two different combinations of power and cost.

All the two–objective computations have been carried out using the $(35, 0, 200)$ EA, with the strength–based cost assignment and without the front thinning option. For the three–objective runs, the $(50, 0, 350)$ EA was used. The thinning of the archival front was activated with an upper bound $\alpha = 400$. The decision variables were coded in

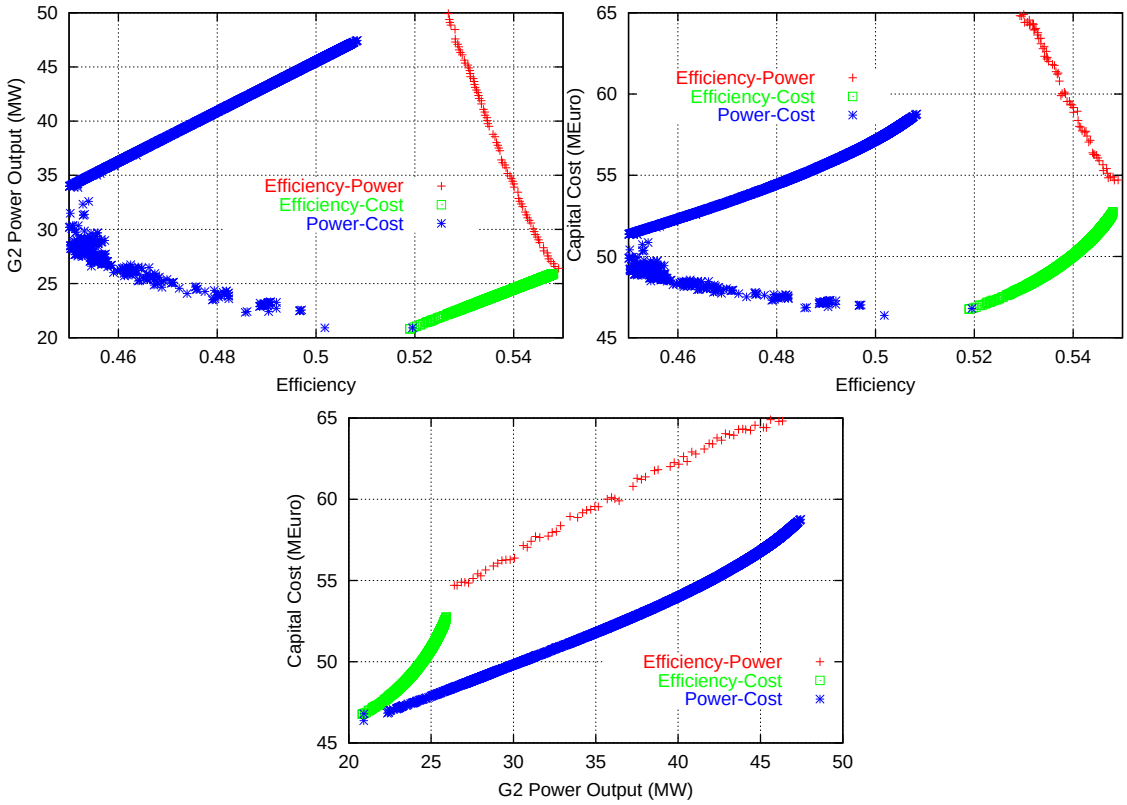

Figure 3: Pareto fronts from two–objective computations, (*max.efficiency–max.power*, *max.efficiency–min.cost* and and *max.power–min.cost*) plotted using *efficiency–power*, *efficiency–cost* and and *power–cost* axes.

binary form using 10 bits per variable. Additionally Gray code was applied to improve the convergence properties. A two–point crossover operator was applied to each pair of parents with probability equal to 90%. The crossover operator affected each pair of decision variables separately from the other ones. The mutation probability was set to 1.9% and was kept constant during the evolution.

Fig. 4 can shed more light to the physical characteristics of the Pareto optimal solution obtained through the two–objective optimizations. Two of the most important design variables, namely the *HP* values and the percentage of the O_2 (of the turbine flue gases) used for the supplementary firing, are plotted. The correspondance of points between figs. 3 and 4 can readily be found. Concerning the *HP* levels, it is interesting to note that the Pareto optimal solutions scan the entire search space for this variable, from 20 up to 100 *bar*. Note, however, that the *efficiency–power* optimization favors configurations operating at the highest *HP* level. Despite the fact that the level of supplementary firing was practically left unbounded (the O_2 percentage was allowed to vary between 0% and 100%), the maximum attained value was close to 10%. This is attributed to the upper bound (565^oC) imposed to the temperature at the steam turbine inlet. It

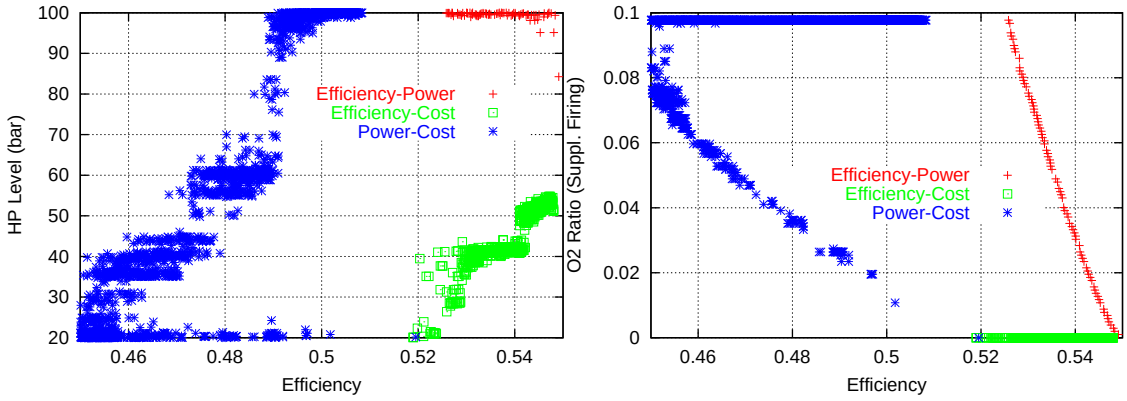

Figure 4: Pressure values at the *HP* branch of the*HRSG* (left) and percentages of the exhaust gas O_2 used for supplementary firing (right) for the two–objective Pareto optimal solutions.

can also be noticed that the *max.efficiency–min.cost* optimization favors configurations without supplementary firing; in contrast, the major part of the Pareto front computed with *max.power–min.cost* targets corresponds to the higher allowed level of supplementary firing.

Some comments on the obtained results may contribute to the understanding of the proposed optimal configurations. For instance, it is clear from fig. 3 (bottom row) that the same power can be achieved with two different capital costs. Using also fig. 4, it comes out that these two solutions correspond to different levels of supplementary firing. In particular, the less expensive solution is the one with maximum use of supplementary firing which, however, yields lower efficiency. Of course, the final choice of the optimal power plant configuration requires a detailed economical analysis, by considering both capital and operating (fuel) costs. To this end, it is interesting to compare two realistic configurations: The capital cost for a plant delivering 35 MW (to the steam turbine generator) is about either 52 $MEuro$ with 45.5% efficiency and 10% supplementary firing or 60 $MEuro$ with 53.8% efficiency and 4% supplementary firing. Thus, in this case, an increase of about 15.4% in capital cost results to about 18.2% higher efficiency. A similar analysis for 45 MW power output gives only 6% higher efficiency while increasing the capital cost by 14%.

Figs. 5, 6 and 7 show the temperature operating levels in terms of the exchanged heat, at some characteristic *HRSG* positions. Fig. 5 analyzes the two extreme optimal points on the *max.efficiency–min.cost* Pareto front. From the results shown so far, all these configurations have been obtained without supplementary firing. Though in both configurations the exhaust gas temperature from the *HRSG* is almost the same, the higher efficiency of the configuration shown in fig. 5 (right) is due to the lower temperature difference at the so–called pinch point (at the exit from the *HP* evaporator). Fig. 6 analyzes the extreme points on the upper branch (as shown in fig. 3, top–left) of the *max.power–min.cost* front; this branch corresponds to the maximum allowed supplementary firing (10%). The higher

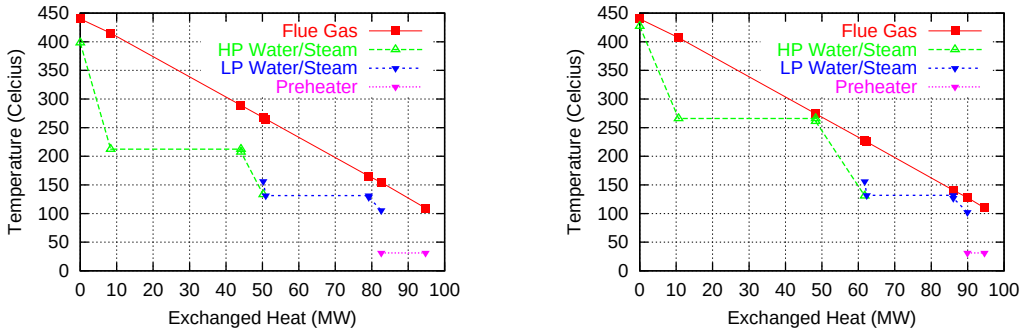

Figure 5: Temperature plots at characteristic locations along the *HRSG*, for the optimal solutions computed through the *max.efficiency–min.cost* optimization. Configuration with minimum (left) and maximum (right) efficiency.

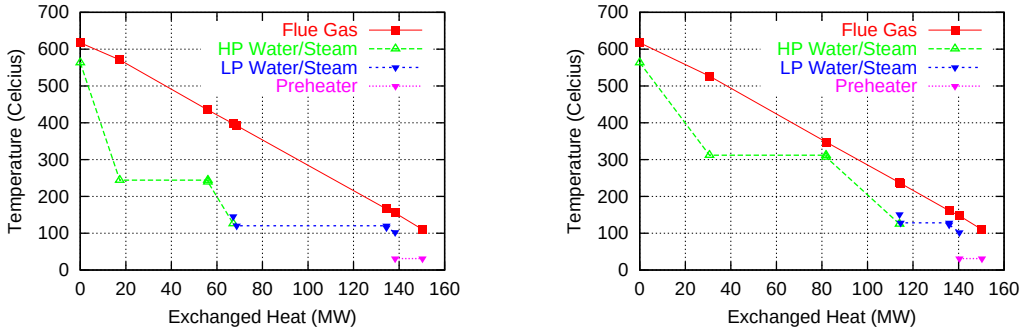

Figure 6: Temperature plots at characteristic locations along the *HRSG*, for the optimal solutions computed through the *max.power–min.cost* optimization. Configuration with minimum (left) and maximum (right) efficiency, for the high–power branch of fig. 3 (upper row,left).

efficiency of the configuration in fig. 6 (right) is due to the same reason (pinch point) as previously exposed.

Fig. 7 corresponds to two optimal configurations resulted from the *max.power–min.cost* optimization, for the same efficiency (50%). The use of 10% supplementary firing (right) yields more than twice the same steam turbine output (with only 23% additional capital cost) thanks to the higher temperatures occuring in the *HRSG*.

6 CONCLUSIONS

An *EA*–based optimization tool (*EASY 1.3*) was utilized for the design of optimal *CCGT* power plants. Using a combination of three– and two–objective analyses, a full understanding of the obtained solutions and the role of supplementary firing was obtained.

CCGT power plant configurations with no supplementary firing are characterized by directly proportional efficiency–power–cost relationships. By introducing supplementary firing, power becomes inversely proportional to the efficiency. The demand for high efficiency–high power output can be met through any percentage of O_2 of the fluw gases

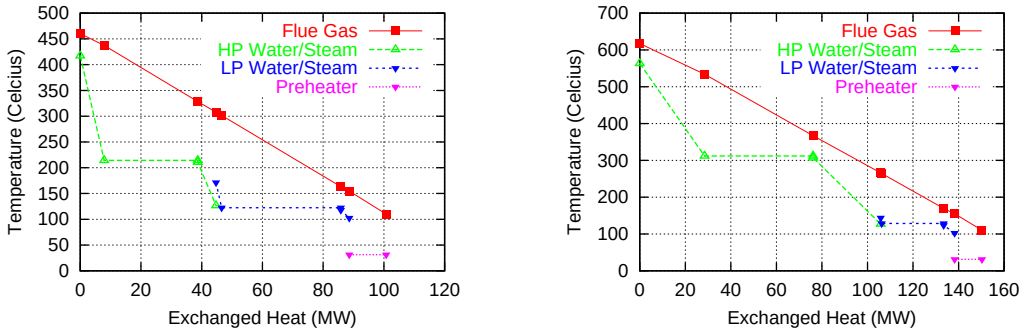

Figure 7: Temperature plots at characteristic locations along the *HRSG*, for the optimal solutions computed through the *max.power–min.cost* optimization. Two configuration with the same efficiency and minimum (left) and maximum (right) power output.

used for supplementary firing (up to its maximum value allowed by the maximum allowed temperature at the steam turbine inlet) but only for the highest pressure level at the *HP* part of the steam cycle. The capital cost is always proportional to the power output. Further decisions about a new *CCGT* power plant can be taken only if the operating cost is taken into account, too.

REFERENCES

[1] K.C. Giannakoglou, A.P. Giotis, and M.K. Karakasis. Low–cost genetic optimization based on inexact pre–evaluations and the sensitivity analysis of design parameters. *Journal of Inverse Problems in Engineering*, 9:389–412, 2001.

[2] K.C. Giannakoglou. Design of optimal aerodynamic shapes using stochastic optimization methods and computational intelligence. *Progress in Aerospace Sciences*, 38:43–76, 2002.

[3] D.E. Goldberg. *Genetic Algorithms in search, optimization & machine learning.* Addison-Wesley, 1989.

[4] Z. Michalewicz. *Genetic Algorithms + Data Structures = Evolution Programs.* Springer-Verlag, Berlin Heidelberg, 2nd edition, 1994.

[5] Th. Back. *Evolutionary Algorithms in Theory and Practice. Evolution Strategies, Evolutionary Programming, Genetic Algorithms.* Oxford University Press, 1996.

[6] N Srinivas and K. Deb. Multiobjective optimization using nondominated sorting in genetic algorithms. *Evolutionary Computation*, pages 221–248, 1994.

[7] C.M. Fonseca and P.J. Fleming. An overview of evolutionary algorithms in multiobjective optimization. *Evolutionary Computation*, 3(1):1–16, 1995.

[8] J. Horn and N. Nafpliotis. Multiobjective optimization using the Niched Pareto Genetic Algorithm. Technical Report IlliGAL 93005, University of Illinois at Urbana-Champaign, Illinois, USA, 1993.

[9] E. Zitzler, K. Deb, and L. Thiele. Comparison of multiobjective evolutionary algorithms: Empirical results. TIK-Report No. 70, Computer Engineering and Communication Networks Lab, ETH Zurich, 1999.

[10] E. Zitzler and L. Thiele. An evolutionary algorithm for multiobjective optimization: The strength Pareto approach. TIK-Report No. 43, Computer Engineering and Communication Networks Lab, ETH Zurich, 1998.

[11] E. Zitzler, M. Laumanns, and L. Thiele. SPEA2 improving the Stength Pareto evolutionary algorithm. TIK-Report No. 103, Computer Engineering and Communication Networks Lab, ETH Zurich, 2001.

[12] E.T. Bonataki and K.C. Giannakoglou. An automated tool for single– and multi–objective optimization for redesigning combined cycle gas turbine power plants. Proceedings of the Fourth GRACM Conference on Computational Mechanics, Patras, Greece, June 2002.